DALTON
FULL PAPER

Lanthanide triple-stranded helical complexes with a substituted 2,6-pyridinedicarboxylate †

Carlos Platas-Iglesias,[a,b] Claude Piguet,[c] Nicolas André[a] and Jean-Claude G. Bünzli *[a]

[a] *Institute of Inorganic and Analytical Chemistry, BCH, University of Lausanne, CH-1015 Lausanne, Switzerland*
[b] *Departamento de Química Fundamental, Universidade da Coruña, Campus de A Zapateira s/n, 15071 A Coruña, Spain*
[c] *Department of Inorganic, Analytical and Applied Chemistry, University of Geneva, 30 quai E. Ansermet, CH-1211 Geneva 4, Switzerland*

Received 21st May 2001, Accepted 3rd August 2001
First published as an Advance Article on the web 1st October 2001

A 4-aminophenylethynyl substituent has been grafted into the 4-position of the pyridine ring in dipicolinic acid to yield ligand L^4 the pK_a's of which are 8.77(5), 3.54(3), 2.58(1) and 1.01(3). Ligand L^4 reacts with trivalent lanthanide ions to give stable triple-stranded helical complexes in water ($\log\beta_{13} = 13.7(1)$ for Eu). The separation of the contact and pseudocontact contributions to the NMR paramagnetic shifts according to the crystal field independent method points to a single axial structure for $[Ln(L^4 - 2H)_3]^{3-}$ along the series Nd–Yb. The solution structure generated by using the dipolar shifts compares well with that reported for the Eu^{III} tris(dipicolinate), with a co-ordination polyhedron which can be described as a distorted tricapped trigonal prism. This is confirmed by a photophysical study of the Eu^{III} complex both in solution and in the solid state. The triplet state of co-ordinated L^4 lies at low energy (around 18 000 cm^{-1} in water) resulting in a relatively poor sensitisation of Eu^{III} (quantum yield *ca.* 0.1% in methanol, lower in water) but in a sizable energy transfer to Yb^{III}.

Introduction

Lanthanide co-ordination compounds[1] continue to receive much attention owing to their important applications as contrast agents for NMR imaging,[2] catalysts for RNA hydrolysis,[3] active agents in cancer radiotherapy,[4] or as luminescence stains in bioanalyses and medical diagnostic.[5] In recent years, we have developed a research program based on the induced fit concept[6] to prepare mono- and di-metallic functional edifices.[7] Our strategy involves the use of aromatic tridentate units derived either from dipicolinic acid (2,6-pyridinecarboxylic acid)[8] or from bis(benzimidazole)pyridine (Scheme 1). The latter binding units have been successfully introduced into homotopic and heterotopic ligands which strictly self-assemble with Ln^{III} ions to produce triple-stranded cationic $[Ln_2(L)_3]^{6+}$[9,10] or neutral $[Ln_2(L^C - 2H)_3]$[11] f–f helicates as well as triple-stranded d–f heterodimetallic podates $[LnM(L')]^{5+}$ (M = Zn, Fe,[12] Co[13]). In a recent paper we have developed a synthetic strategy for grafting an halogenide substituent onto the pyridine moiety of ligand L to obtain L^E, which can be used as a synthon for additional substitution of the pyridine with more elaborate groups.[10]

Luminescent probes for bioanalytical analyses require assemblies that are stable under physiological conditions, which bear efficient chromophoric groups and which can easily couple with biological molecules. As an alternative to the above strategy, we test here the possibility of grafting adequate substituents in the 4-position of the dipicolinic acid framework, since this tridentate aromatic unit forms stable and strongly luminescent triple-stranded helical $[Ln(L^1 - 2H)_3]^{3-}$ complexes in water[14] or $[Ln(L^{2,3})_3]^{3+}$ edifices in acetonitrile.[15] We have also

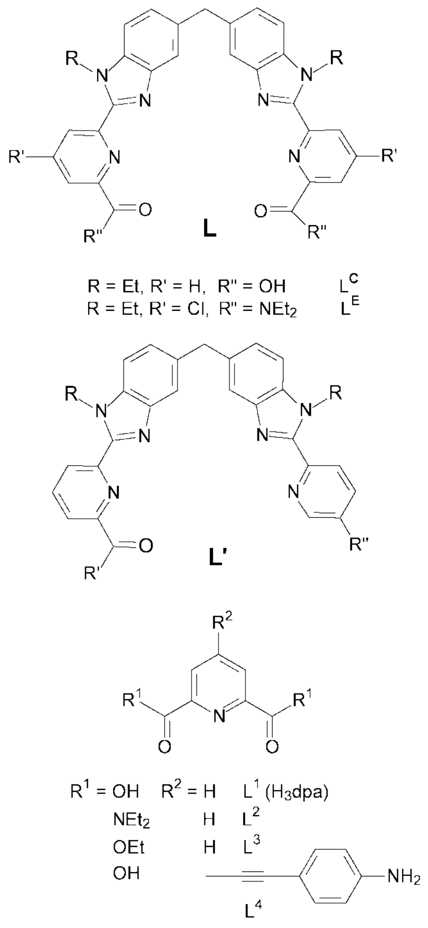

Scheme 1

---

† Electronic supplementary information (ESI) available: analytical, IR and luminescence data, contact and dipolar shifts, calculated Cartesian co-ordinate for the Eu^{III} complex, plots of chemical shifts for protons H^8, H^9 *versus* the chemical shift of proton H^2. See http://www.rsc.org/suppdata/dt/b1/b104448f/

DOI: 10.1039/b104448f

recently demonstrated that the introduction of a bulky chiral substituent in the R^2 position of L^2 does not prevent helical wrapping around the metal ions and leads to the formation of stable complexes in acetonitrile.[16] In another study, Wensel *et al.*[17] have examined the sensitisation of Tb^{III} in water by a series of 4-substituted analogues of dipicolinic acid bearing simple groups (R = NH_2, OH, NHAc, Cl, H or Br). In this work, we introduce a 4-aminophenylethynyl substituent in the 4-position of the pyridine in L^1 to yield L^4. It is expected that electronic delocalisation will induce a relatively low lying triplet state, thus providing energy transfer paths to Eu^{III} and Yb^{III}. We also investigate the solution structure of the resulting 1 : 3 complexes making use of the separation of contact and pseudo-contact contributions to the NMR paramagnetic shifts.

Experimental

Solvents and starting materials

Triethylamine was distilled from CaH_2. Other products were purchased from Fluka AG (Buchs, Switzerland) and used without further purification, unless otherwise stated. The $Na_3[Gd(L^1 - 2H)_3]$ complex was prepared by a similar procedure to that previously described.[14b]

Spectroscopic and analytical measurements

Elemental analyses were carried out on a Carlo Erba EA 1108 elemental analyser. Electronic spectra in the UV-vis range were recorded at 20 °C with a Perkin-Elmer Lambda 7 spectrometer using 1.0 and 0.1 cm quartz cells. In a typical spectrophotometric pH titration, 25 cm^3 of a 1×10^{-5} M solution of L^4 or of a 1.5×10^{-4} M solution of $Cs_3[Eu(L^4 - 2H)_3]$ in water containing 0.05 M $KClO_4$ was prepared, and the starting pH (measured with a Metrohm 6.3013.210 glass electrode) was adjusted with solid Cs_2CO_3. The pH was then progressively decreased with 1 M HCl, the equilibrium being reached almost immediately. The spectrophotometric titration of L^4 with $Eu(ClO_4)_3 \cdot xH_2O$ was performed on a Perkin-Elmer Lambda 900 spectrometer: 25 cm^3 of a 2.53×10^{-5} M solution of L^4 buffered at pH 7.7 with 0.1 M tris/tris·HCl [tris = tris(hydroxymethyl)aminomethane] was prepared, and 0.05 cm^3 aliquots of a 2.68×10^{-4} M solution of $Eu(ClO_4)_3 \cdot xH_2O$ were successively added. For both titrations, plots of the molar absorption coefficient as a function of the pH or M/L ratio as well as factor analysis[18] were used to determine a suitable model, and the data were analysed with the SPECFIT program.[19] Reflectance spectra were recorded as finely ground powders dispersed in MgO (5%) with MgO as the reference on a Perkin-Elmer Lambda 900 spectrometer equipped with a Labsphere PELA-1000 integration sphere. IR spectra were obtained from KBr pellets with a Mattson α-Centauri FT-IR spectrometer. ^1H and ^{13}C NMR spectra were recorded at 25 °C on Bruker AM-360 or Bruker AVANCE 400-DRX spectrometers, and the pD (= pH + 0.4[20]) was adjusted with D_2SO_4 (Fluka) or NaOD (40% in D_2O, Merck). Chemical shifts are reported in parts per million with respect to $SiMe_4$ (referenced to internal HOD at 4.75 ppm). The experimental procedures for high resolution, laser excited luminescence measurements have been published previously.[21] Quantum yields were measured relative to quinine sulfate in 0.05 M H_2SO_4 according to a procedure previously described[22] (n = 1.338, absolute quantum yield: 0.546).[23] The refractive indices used were 1.333 and 1.329 for solutions in H_2O and MeOH, respectively. Ligand excitation and emission spectra were recorded on a Perkin-Elmer LS-50B spectrometer equipped for low temperature (77 K) measurements.

Preparation of the ligand

4-(4-Aminophenylethynyl)pyridine-2,6-dimethylcarboxylate. The compound was prepared by a somewhat different procedure to that previously reported by Takalo and co-workers,[24] from 4-aminophenylacetylene[25] and 4-bromopyridine-2,6-dimethylcarboxylate[17] instead of the corresponding iodine-derivative: 1.124 g of 4-bromopyridine-2,6-dimethylcarboxylate (4.1 mmol), 0.0581 g of bis(triphenylphosphine)palladium(II) chloride (0.082 mmol) and 0.0312 g of copper(I) iodide (0.164 mmol) were suspended in 16 cm^3 of Et_3N and the mixture was stirred under an inert atmosphere (N_2) for 15 min. A 0.480 g amount of 4-aminophenylacetylene (4.1 mmol) was added and the mixture was heated under N_2 for 4 h at 40 °C and then evaporated to dryness. The solid residue was dissolved in CH_2Cl_2 (200 cm^3) and the resultant solution washed with water (30 cm^3). The organic phase was dried over Na_2SO_4, and evaporated to dryness. Methanol (20 cm^3) was added to the residue, a yellow-brown crystalline product appeared which was filtered off under vacuum, washed with MeOH (20 cm^3) and dried under vacuum to get 1.081 g of the desired compound (yield 85%). ^1H-NMR in $(CD_3)_2SO$: δ 8.16 (2H, s), 7.33 (2H, t, ^3J = 8.94 Hz), 6.58 (2H, t, ^3J = 8.93), 5.86 (2H, b), 3.93 (6H, s).

4-(4-Aminophenylethynyl)pyridine-2,6-dicarboxylic acid dichlorohydrate, $L^4 \cdot 2HCl$. A 1.081 g (3.48 mmol) amount of 4-(4-aminophenylethynyl)pyridine-2,6-dimethylcarboxylate was refluxed in 50 cm^3 of a KOH solution 0.1 M in EtOH–H_2O (1 : 1). After completion of the reaction (12 h) the solution was concentrated under vacuum to remove the ethanol and the resulting brown aqueous solution was acidified to pH ≈ 1 with 25% aqueous HCl. The brown precipitate formed was filtered off, washed with water (5 cm^3) and dried under vacuum (10^{-2} Torr) at 75 °C for 12 h to get 0.854 g of the desired product as a pale brown solid (yield 69%) [Found: C, 51.43; H, 3.15; N, 7.92; calc. for $C_{15}H_{10}N_2O_4 \cdot 2HCl$: C, 50.73; H, 3.41; N, 7.89%]. ^1H-NMR in $(CD_3)_2SO$: δ 8.02 (2H, s), 7.36 (2H, d, ^3J = 8.9 Hz), 6.65 (2H, d, ^3J = 8.9). ESI-MS (H_2O): m/z 283 $[M + H]^+$. IR ν(cm^{-1}, KBr): 2200 (C≡C), 1719 (C=O), 1116 (C–O).

Preparation of the $Cs_3[Ln(L^4 - 2H)_3] \cdot xH_2O$ complexes

The perchlorate salts $Ln(ClO_4)_3 \cdot xH_2O$ (x = 6–8) were prepared from the corresponding oxides (Rhône-Poulenc, 99.99%) according to the literature method.[26]

CAUTION: perchlorate salts combined with organic ligands are potentially explosive and should be handled in small quantity and with the necessary precautions.[27]

A 0.030 g amount of $L^4 \cdot 2HCl$ (84.5 μmol) was suspended in methanol (10 cm^3) and Cs_2CO_3 (0.0358 g, 337.9 μmol) were added. The resultant solution was stirred and heated to reflux for 10 min; the corresponding lanthanide perchlorate salt (28.15 μmol) dissolved in 10 cm^3 of the same solvent was added dropwise to the former solution. The resultant yellow solution was stirred and heated to reflux until complete reaction of the carbonate, filtered while hot and evaporated slowly at room temperature. The yellow crystals formed were filtered and dried under vacuum to give $Cs_3[Ln(L^4 - 2H)_3] \cdot nH_2O$ (n = 2–3, Ln = Eu, Gd, Tb) in 70–80% yield. The $[Ln(L^4 - 2H)_3]^{3-}$ complexes used for NMR measurements (Ln = Nd, Tb, Dy, Ho, Er, Tm, Lu, Y) were prepared by the same procedure, but were not crystallised.

Results and discussion

Synthesis and properties of the ligand and its lanthanide complexes

4-(4-Aminophenylethynyl)pyridine-2,6-dicarboxylic acid (L^4) was obtained in good overall yield from commercially available products by a four-step procedure involving a Sonogashira[28] type coupling reaction as the key step for the substitution of the pyridine 4-position (Scheme 2). At pH = 10.74, $[L^4 - 2H]^{2-}$

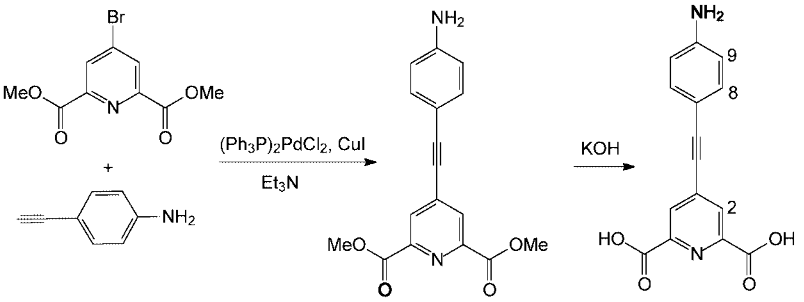

Scheme 2

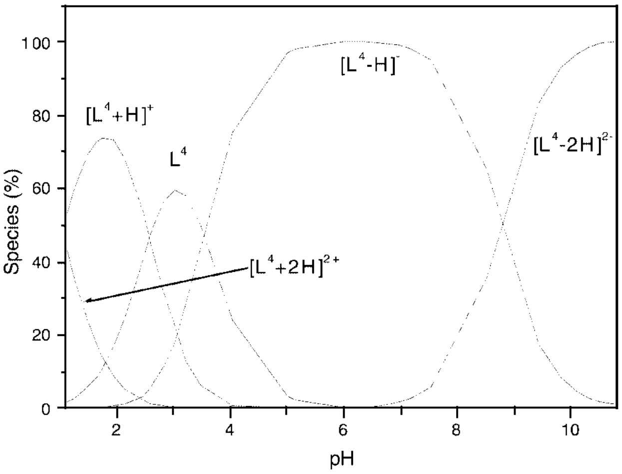

Fig. 1 Distribution diagram for L^4.

presents two main absorption bands at 29 918 and 38 760 cm^{-1}, assigned to $\pi \longrightarrow \pi^*$ transitions mainly located on the 4-aminophenylethynyl and pyridine moieties, respectively. A spectrophotometric titration of a 10^{-5} M aqueous solution of $[L^4 - 2H]^{2-}$ with hydrochloric acid (starting pH = 10.76) revealed four different equivalence points corresponding to $pK_{a1} = 8.77 \pm 0.05$, $pK_{a2} = 3.54 \pm 0.03$, $pK_{a3} = 2.58 \pm 0.01$ and $pK_{a4} = 1.01 \pm 0.03$. The distribution curves of the different species are shown in Fig. 1. The highest protonation constant corresponds to the protonation of the amine group, while the second represents the protonation of the pyridine nitrogen, the latter value being *ca.* 10 times smaller than for dipicolinic acid ($pK_a = 4.63$,[29] 4.76[30]), probably as a consequence of the reduced negative charge in $[L^4 - H]^-$ compared to $[L^1 - 2H]^{2-}$. Finally, the last two protonation steps with a ΔpK_a of 1.57 correspond to the protonation of the carboxylic functions. As the expected statistical separation for two non-interacting carboxylic groups belonging to the same molecule is $\Delta pK_a = 0.6$,[31] the larger ΔpK_a value observed for L^4 points to the two carboxylic groups interacting through intramolecular hydrogen bond(s) in the $[L^4 + H]^+$ species.

Reaction of stoichiometric amounts of $L^4{\cdot}2HCl$, Cs_2CO_3 and the corresponding hydrated lanthanide perchlorate (Ln = Eu, Gd, Yb) gives yellow-orange solutions in methanol from which the $Cs_3[Ln(L^4 - 2H)_3]{\cdot}nH_2O$ complexes can be isolated in 70–80% yield (Table S1, ESI). These complexes present a number of identifying IR bands including (see Table S1, ESI): (i) intense carbonyl symmetric and asymmetric stretching vibrations at 1590 and 1616 cm^{-1}, respectively, (ii) an intense C≡C stretching vibration at *ca.* 2200 cm^{-1}, and (iii) uncoordinated water molecules at 3400 cm^{-1}. Moreover, the absence of any absorption band arising from the perchlorate group unambiguously proves the displacement of the anion during the formation of the complexes. At pH 10.4 the $[Ln(L^4 - 2H)_3]^{3-}$ complexes present two main absorption bands (Table 1), which are shifted to lower energies compared to those of $[L^4 - 2H]^{2-}$. In complete contrast with the free ligand, the absorption spectra of a 1.5×10^{-4} M aqueous solution of $[Eu(L^4 - 2H)_3]^{3-}$ remain unchanged in the pH range 5.00 < pH < 10.4, while dissociation of the complex occurs at pH < 5.0. Upon complexation, the $\pi \longrightarrow \pi^*$ transition of L^4 appearing at higher energy undergoes a red shift of *ca.* 1750 cm^{-1}, thus enabling the monitoring of the complex formation.

Spectrophotometric titration of L^4 with $Eu(ClO_4)_3{\cdot}xH_2O$ was performed in aqueous solution buffered at pH 7.7. Plots of the molar absorption coefficient *versus* the ligand/metal ratio at different wavelengths show a break for the 3 : 1 complex, the spectrum remaining then unchanged until the ligand/metal ratio reaches 1.35 : 1. This result was confirmed by factor analysis and the data could be satisfactorily fitted to equilibrium (1) allowing an estimation of the overall stability constant: $\log(\beta_{13}^{Eu}) = 13.7(1)$. Protonation of the amine group of L^4 was not taken into account for the sake of simplicity.

$$3\,(L^4 - 2H)^{2-} + Eu^{3+} \rightleftharpoons [Eu(L^4 - 2H)_3]^{3-} \quad \log(\beta_{13}^{Eu}) \qquad (1)$$

This result should be taken with care, since precipitation occurs for ligand/metal ratios < 1.35 : 1, preventing a complete analysis allowing for the formation of the 1 : 1 and 1 : 2 species. Nevertheless, the $\log(\beta_{13}^{Eu})$ value points to an important decrease in the stability of the $[Ln(L^4 - 2H)_3]^{3-}$ complexes compared to $[Ln(L^1 - 2H)_3]^{3-}$, for which $\log(\beta_{13}^{Ln})$ is in the range 18–22.[15a] This can be tentatively assigned to a larger electron delocalisation onto the extended π system of L^4, but partial protonation of the terminal amino groups leading to reduced electrostatic Ln–ligand interactions in $[Ln(L^4 - 2H + nH)_3]^{(3-n)-}$ cannot be excluded at pH = 7.7.

Solution structure of $[Ln(L^4 - 2H)_3]^{3-}$ complexes

The structure of the $[Ln(L^4 - 2H)_3]^{3-}$ complexes was studied in D_2O by ^1H NMR spectroscopy, since the low solubility of the complexes prevents recording the ^{13}C spectra. The spectra of the Y and Lu diamagnetic complexes (Table 2) show the expected simple pattern with three signals corresponding to the three non-equivalent aromatic protons of the three equivalent ligand strands. The signal due to the H^2 protons shifts to higher field by 0.11 ppm upon complexation, while the signals of the H^8 and H^9 protons are less affected. The ^1H NMR shifts of the paramagnetic complexes are also listed in Table 2, as measured at 6 < pD < 8. A detailed study of a 10^{-3} M aqueous solution of $[Eu(L^4 - 2H)_3]^{3-}$ *vs.* the pD shows the ^1H shifts being completely pD-independent between 5.7 and 10.3, suggesting that the Eu^{III} complex presents a single solution structure in this pD range, in agreement with the UV-visible data (*vide supra*).

Finer structural information can be gained from the separation of the contact (δ_{ij}^{c}) and pseudocontact contributions (δ_{ij}^{pc}) to the isotropic paramagnetic shift (δ_{ij}^{para})[32] of a nucleus *i* induced by a lanthanide ion *j* (LIS):

$$\delta_{ij}^{para} = \delta_{ij}^{exp} - \delta_{i}^{dia} = \delta_{ij}^{c} + \delta_{ij}^{pc} = F_i\langle S_z\rangle_j + G_iC_j \qquad (2)$$

where F_i is the hyperfine coupling constant of nucleus *i*, which governs the contact interaction between that nucleus and

Table 1 Ligand-centred absorption and emission properties of L^4 and $[Ln(L^4-2H)_3]^{3-}$

Compound	$E(\pi\longrightarrow\pi^*)^a$/cm^{-1}	Solvent	$E(\pi\longrightarrow\pi^*)^b$/cm^{-1}	$E(^1\pi\pi^*)^d$/cm^{-1}	$E(^3\pi\pi^*)^e$/cm^{-1}	$\tau(^3\pi\pi^*)^e$/ms
L^4	29 233	H_2O^c	29 918 (4.16)	22 844		
	36 605		38 760 (4.04)			
		MeOH	27 585 (4.15)	19 176	18 727	
			37 678 (4.03)			
Eu	28 203	H_2O^c	28 169 (4.68)	20 175		
	35 540		38 168 (4.01)			
			46 125 (4.70)			
		MeOH	27 585 (4.08)		^{f}	^{f}
			37 678 (4.00)			
			47 092 (4.20)			
Gd	27 864	H_2O^c	28 558 (4.67)	18 132	17 555	1.54 ± 0.03
	35 540		38 121 (4.59)			
			46 685 (4.77)			
		MeOH	27 777 (4.64)	19 656	18 198	1.86 ± 0.09
			37 594 (4.51)			
			46 729 (4.72)			

[a] Reflectance spectra recorded at 295 K. [b] Electronic spectral data at 295 K; energies are given for the maximum of the band envelope in cm^{-1}; log ε is given within parentheses. [c] Buffered solution (pH = 8.0). [d] From luminescence data in solution at 295 K. [e] Luminescence data and lifetimes in frozen solutions at 77 K. [f] $^3\pi\pi^*$ Luminescence quenched by transfer to the lanthanide ion.

Table 2 ^{1}H-NMR shifts (ppm) for L^4 (pD = 12.0) and for the $[Ln(L^4-2H)_3]^{3-}$ complexes in D_2O ($7.4 < pD < 8.4$) at 298 K, and relevant data for the analysis of the paramagnetic shifts

Compound	H^2	H^8	H^9	$AF_j{}^c$	$AF_j{}^d$	$AF_j{}^e$
$(L^4-2H)^{2-}$	7.95	7.41	6.77			
Y	8.06	7.44	6.78			
Nd	10.49	7.88	6.98	0.2800	0.0065	0.1368
Eu	3.89	6.75	6.48	0.0519	0.0067	0.1364
Tb	41.52	15.47	11.38	0.1420	0.0055	0.1388
Dy	44.92	16.09	11.69	0.0300	0.0056	0.1387
Ho	27.34	13.27	10.29	0.0189	0.0153	0.1404
Er	−2.38	5.41	5.60	0.0503	0.0154	0.1407
Tm	−13.89	3.04	4.37	0.0881	0.0151	0.1407
Yb	0.04	5.64	5.79	0.0453	0.0150	0.1400
Lu	8.06	7.39	6.73			
Nd to Dy				H^9–H^2	H^9–H^8	H^8–H^2
F_i	0.29(7)	0.03(1)	0.008(5)			
G_i	0.44(3)	0.096(5)	0.052(3)			
$AF_i{}^c$	0.1009	0.0630	0.0580			
$R_{ik}{}^a$				0.118	0.542	0.218
Ho to Yb				H^9–H^2	H^9–H^8	H^8–H^2
F_i	−0.16(4)	−0.089(8)	−0.057(8)			
G_i	0.40(3)	0.092(3)	0.0512(3)			
$AF_i{}^c$	0.0631	0.0590	0.0968			
$R_{ik}{}^a$				0.128	0.557	0.230
Nd to Yb	H^9–H^2	H^9–H^8	H^8–H^2			
$R_{ik}{}^b$	0.122(4)	0.552(6)	0.221(6)			
$(F_i-R_{ik}F_k)^b$	−0.025(6)	−0.007(2)	−0.032(9)			

[a] $R_{ik} = G_i/G_k$, with G_i and G_k obtained according to eqn. (4) and (5). [b] According to eqn. (7). [c] Reilley's analysis, eqn. (6). [d] Calculated shifts estimated by the SHIFT ANALYSIS program[42] with assignment shown (see text). [e] Calculated shifts estimated by the SHIFT ANALYSIS program[42] with inverted assignment for H^8 and H^9 (see text).

the Ln_j ion and G_i is the geometric factor of nucleus i containing the structural information, $\langle S_z\rangle_j$ and C_j are, respectively, the spin expectation value and the magnetic constant (Bleaney factor) of the paramagnetic lanthanide. The diamagnetic contribution δ_i^{dia} is obtained by measuring chemical shifts for isostructural diamagnetic complexes: $[Y(L^4-2H)_3]^{3-}$ was used for the earlier (Nd–Dy) and $[Lu(L^4-2H)_3]^{3-}$ for the later (Ho–Yb) members of the lanthanide series. For a complex with effective axial magnetic symmetry,[33]

$$G_i = \frac{A_2^0\langle r^2\rangle}{T^2} \times \frac{1-3\cos^2\theta_i}{r_i^3} \tag{3}$$

where $A_2^0\langle r^2\rangle$ is the second-order axial crystal field parameter, which is a measure of the strength of interaction between a given lanthanide ion and the ligand donor atoms, and r_i and θ_i are the internal axial co-ordinates of nucleus i with respect to the ligand field axis. A straightforward separation of the contact term F_i and the pseudo-contact term G_i for each nucleus i in the axial lanthanide complexes $[Ln(L^4-2H)_3]^{3-}$ can be performed by rearranging eqn. (2) into the linear forms given by eqn. (4) and (5):

$$\frac{\delta_{ij}^{\mathrm{para}}}{\langle S_Z\rangle_j} = F_i + G_i\frac{C_j}{\langle S_z\rangle_j} \tag{4}$$

$$\frac{\delta_{ij}^{\mathrm{para}}}{C_j} = G_i + F_i\frac{\langle S_z\rangle_j}{C_j} \tag{5}$$

Assuming that $\langle S_z\rangle_j$ and C_j values are the same for the complexes and the free ions,[34] for which they are tabulated,[35,36] plots of $\delta_{ij}^{\mathrm{para}}/\langle S_z\rangle_j$ against $C_j/\langle S_z\rangle_j$ and of $\delta_{ij}^{\mathrm{para}}/C_j$ against $\langle S_z\rangle_j/C_j$ should be linear with a slope equal to G_i and F_i, respectively, if the complexes are isostructural and possess comparable crystal field parameters. The pseudocontact and contact contributions

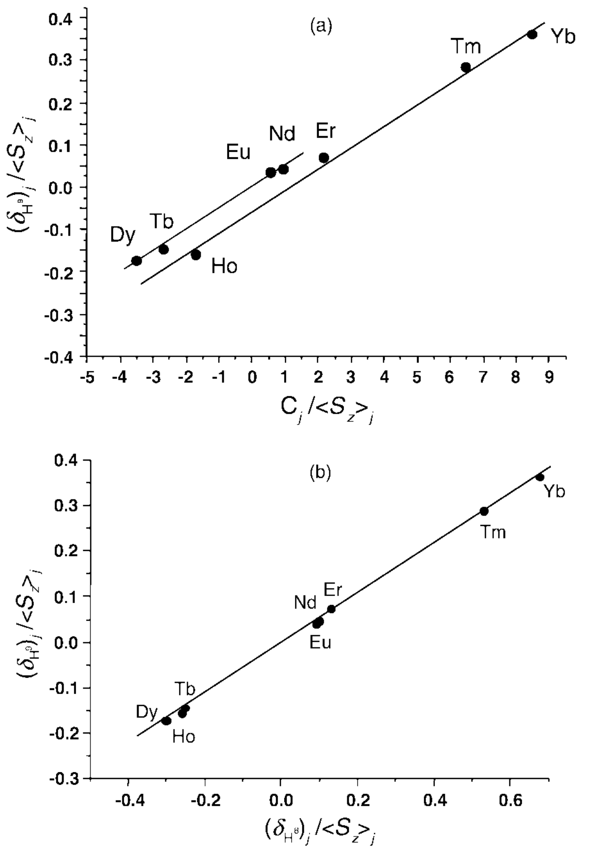

Fig. 2 Plots of: (a): $\delta_{ij}^{\text{para}}/\langle S_z\rangle_j$ *vs.* $C_j/\langle S_z\rangle_j$ for H^9 according to eqn. (4) and (b): $\delta_{ij}^{\text{para}}/\langle S_z\rangle_j$ *vs.* $\delta_{kj}^{\text{para}}/\langle S_z\rangle_j$ ($i = H^9$, $k = H^8$) according to eqn. (7) for $[Ln(L^4 - 2H)_3]^{3-}$ 10^{-3} M in D_2O at 298 K.

to the observed LIS separated by using eqn. (4) and (5) are reported in Table 2 along with the agreement factors AF_i and AF_j (eqn. (6); see also Table S2, ESI). The resulting plots fall

$$AF_i = \left[\sum_j (\delta_{ij}^{\exp} - \delta_{ij}^{\text{cal}})^2 / \sum_j (\delta_{ij}^{\exp})^2\right]^{1/2} \text{ and}$$
$$AF_j = \left[\sum_i (\delta_{ij}^{\exp} - \delta_{ij}^{\text{cal}})^2 / \sum_i (\delta_{ij}^{\exp})^2\right]^{1/2} \quad (6)$$

into two groups (Ln = Nd–Dy and Ln = Ho–Yb) with a break near the middle of the series as illustrated in Fig. 2a for H^9. In principle, such a situation may point to the $[Ln(L^4 - 2H)_3]^{3-}$ helicates being not isostructural. However, deviation from linearity also occurs because of variation in the crystal field parameter[37] or in both this parameter and the hyperfine coupling constant F_i.[38,39] In our case, since two straight parallel lines are observed we can infer that: (i) the complexes are most probably isostructural along the lanthanide series, (ii) the crystal field parameter remains invariant along the lanthanide series, but (iii) a change occurs in the contact terms along the lanthanide series and is responsible for the break. The agreement factors calculated for both series, $0.058 < AF_i < 0.101$ (Nd–Dy) and $0.059 < AF_i < 0.097$ (Ho–Yb), are comparable to those found for $[Ln(L^1 - 2H)_3]^{3-}$ [34] and 4f–4f[11] helicates. The contact contributions are relatively small for all the protons, F_i reaching a significant value only for H^2, which points to a sizeable spin density delocalisation onto the pyridine ring.

Recently, Platas *et al.*[38] proposed a crystal-field independent method, which allows the rationalisation of the origin of some of the breaks found in the plots according to eqn. (4) and (5), by simultaneously solving eqn. (2) for two different nuclei *i* and *k*:

$$\frac{\delta_{ij}^{\text{para}}}{\langle S_z\rangle_j} = (F_i - R_{ik}F_k) + R_{ik}\frac{\delta_{kj}^{\text{para}}}{\langle S_z\rangle_j}, \quad R_{ik} = G_i/G_k \quad (7)$$

The three plots according to eqn. (7) involving the H^2, H^8 and H^9 protons display a single straight line (Nd–Yb, Fig. 2b), and yield R_{ik} values in excellent agreement with those calculated from eqn. (4) and (5) (Table 2), confirming a single structure along the series (Nd–Yb) and also that a change in the hyperfine coupling constant is responsible for the breaks found in the plots according to eqn. (4) and (5). This behaviour contrasts with that of the $[Ln(L^2)_3]^{3+}$ complexes, which show two different structural series for Ln = Ce–Tb and Ln = Er–Yb.[39] As eqn. (7) takes into account the paramagnetic shift for two nuclei *i* and *k*, two new agreement factors characteristics of the fitting process and related to a given proton (eqn. (8)) or a given lanthanide ion (eqn. (9)) can be calculated:

$$AF_{i,k} = \left[\sum_j (\delta_{ij}^{\exp}) - (\delta_{ij}^{\text{cal}} f(\delta_{kj}^{\exp}))^2 / \sum_j (\delta_{ij}^{\exp})^2\right]^{1/2} \quad (8)$$

$$AF_{j,k} = \left[\sum_i (\delta_{ij}^{\exp}) - (\delta_{ij}^{\text{cal}} f(\delta_{kj}^{\exp}))^2 / \sum_i (\delta_{ij}^{\exp})^2\right]^{1/2} \quad (9)$$

Where $\delta_{ij}^{\text{cal}} f(\delta_{kj}^{\exp})$ is defined as the paramagnetic shift for nucleus *i* calculated from eqn. (7) by using the experimental paramagnetic shift for nucleus *k*. The extracted agreement factors (Table S3, ESI) are globally satisfactory and are in line with the AF_i's and AF_j's obtained for the plots according to eqn. (4) and (5). However, we notice that the use of $\delta_{ij}^{\text{cal}} f(\delta_{9j}^{\exp})$ for H^9 and, in a less drastic proportion, for H^8 as references produce poor predictions according to eqn. (7) for the weakly paramagnetic ions Nd^{III} and Eu^{III}. This may be explained by the fact that these remote protons undergo only small paramagnetic induced shifts and, therefore, the division by small $\Sigma(\delta_{ij}^{\exp})^2$ quantities leads to large $AF_{i,k}$'s and $AF_{j,k}$'s for these ions.

We have also used the dipolar shifts to generate the structure of the $[Ln(L^4 - 2H)_3]^{3-}$ complexes in aqueous solution, which requires an initial estimate of this structure. It is well known that $[Ln(L^1 - 2H)_3]^{3-}$ complexes present a somewhat distorted D_3 symmetry in the solid state with a co-ordination polyhedron around the lanthanide ion close to a tricapped trigonal prism.[14b,c] On the other hand, circularly polarised luminescence studies are consistent with a D_3 symmetry in solution, the complexes existing as a racemic mixture of Λ and Δ enantiomeric structures.[40] Since luminescence data demonstrate that the $[Eu(L^4 - 2H)_3]^{3-}$ complex also displays D_3 symmetry in solution (see below), we have taken the X-ray structure of the $[Eu(L^1 - 2H)_3]^{3-}$ complex as a reasonable starting model for the structure of $[Eu(L^4 - 2H)_3]^{3-}$. The 4-aminophenylethynyl substituent was then introduced using the molecular mechanics program Cerius-2[41] in the following way: the co-ordinates of the donor atoms were fixed and the molecule let to relax, yielding a first set of Cartesian co-ordinates. The C_3 axis of symmetry, taken as the *z*-axis, was assumed to go through the metal ion and one of the three triangular faces of the trigonal prism formed by three carboxylate O atoms. One of the Ln–N vectors was set as the *y* axis. Finally, the $Ln(L^4 - 2H)$ unit with the pyridine nitrogen atom situated on the *y* axis was used to estimate the idealised Ln–donor distances with the SHIFT ANALYSIS program:[42] the principal magnetic axis of symmetry was taken as the *z* axis, the Ln ion was moved along the *y* axis and plots of the agreement factor AF_j (eqn. (6)) *vs.* the Ln–N bond distance revealed minima that best fit the LIS data (Fig. 3). The obtained idealised Ln–N and Ln–O distances were 2.57 and 2.46 Å, respectively, in good agreement with the averaged distances found for $[Eu(L^1 - 2H)_3]^{3-}$ in the solid state (2.54 and 2.45 Å, respectively).[14c] In a last step, the resulting Cartesian co-ordinates obtained from the optimisation of the Ln–donor distances (Table S4, ESI) were used, after transformation into cylindrical (r, θ, z) co-ordinates and assuming trigonal symmetry, to generate the best structural model for the

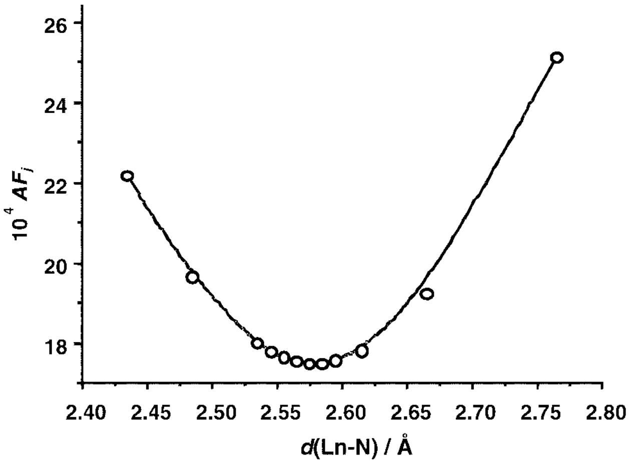

Fig. 3 Plot of the agreement factor AF_j *vs.* the Ln–N bond distance for $[Eu(L^4 - 2H)_3]^{3-}$ in D_2O.

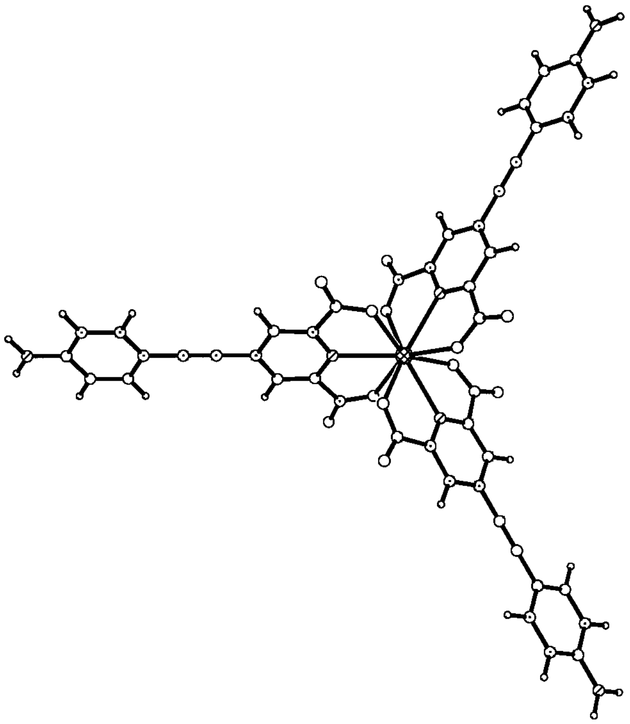

Fig. 4 Perspective view of one of the two helical forms of the $[Ln(L^4 - 2H)_3]^{3-}$ complex in D_2O solution as determined from the ^{1}H-NMR data.

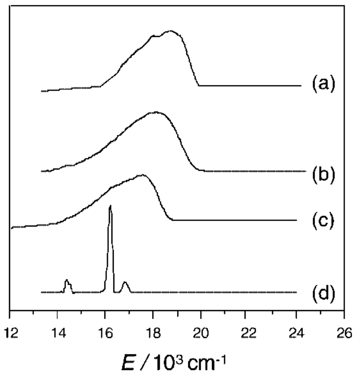

Fig. 5 Phosphorescence spectra at 77 K for: (a) L^4 in frozen methanol solution; (b) $[Gd(L^4 - 2H)_3]^{3-}$ in frozen methanol solution; (c) $[Gd(L^4 - 2H)_3]^{3-}$ in frozen water solution; (d) $[Eu(L^4 - 2H)_3]^{3-}$ in frozen methanol solution.

complexes in solution (Fig. 4). The cylindrical co-ordinates were transformed back into Cartesian co-ordinates (Table S4, ESI), and the SHIFT ANALYSIS program was used to calculate the agreement factor between the experimental and calculated shifts. The resulting agreement factor $AF_j = 0.00668$ is excellent. The generated co-ordination polyhedron is a tricapped trigonal prism which can be considered as being comprised of three tripods defining three parallel planes: the O atoms from the carboxylates define the upper and lower tripods, while the N atoms of the pyridine moieties delineate the capping tripod, the lanthanide ion lying at the centre of the latter tripod. The distance between the facial planes of the distal tripods is 3.22 Å, comparable to that observed for $[Eu(L^1 - 2H)_3]^{3-}$ in the solid state (3.33 Å). The angle between the projection vectors of the two distal tripods on the plane formed by the capping tripod and the lanthanide ion amounts to 15.8° for the $[Eu(L^4 - 2H)_3]^{3-}$ complex, pointing to a certain degree of distortion from the ideal geometry (angle 0°) but compares well with the average value found in the solid state for $[Eu(L^1 - 2H)_3]^{3-}$ (15.6°),[14c] despite the reduced number of experimental data at hand to refine the solution structure.

Finally, we have checked the assignment for protons H^8 and H^9 by using the SHIFT ANALYSIS program[42] and the above-calculated geometry to test an interchange of attribution between these two protons for each Ln^{III} ion. The calculated pseudocontact contributions to the LIS match those extracted from Reilley's analysis when the attribution of Table 2 is taken into consideration, which is not the case for the inverted assignment. This is reflected in the corresponding AF_i's calculated according to eqn. (6) and reported in Table 2. It is noteworthy that plots of the chemical shifts of H^8 and H^9 assigned according to Table 2 *versus* the chemical shift of H^2, the assignment of which is unambiguous, are linear, reflecting both the correctness of the H^8 and H^9 signal assignment and the isostructurality within the series (Fig. S1, ESI).

Photophysical properties

The emission spectrum of L^4 in methanolic solution (295 K) under excitation at 25 253 cm^{-1} presents a single weak emission band (Table 1) the intensity of which quickly diminishes when a short delay (0.1 ms) is enforced and this band is therefore attributed as arising from the $^1\pi\pi^*$ state. In aqueous solution the $^1\pi\pi^*$ emission appears at higher energy and is nearly pH-independent in the range 5.6–10.9, in complete contrast with the absorption spectra. The emission spectrum recorded in frozen methanolic solution (77 K, delay 0.10 ms) presents a second band with a maximum at 18 730 cm^{-1} which is assigned as arising from to the $^3\pi\pi^*$ state (Fig. 5). Upon complexation to the Gd^{III} ion the ligand-based triplet state emission undergoes a red shift of 529 cm^{-1} (MeOH) or 643 cm^{-1} (H_2O). The introduction of a 4-aminophenylethynyl substituent affects drastically the energy of the $^3\pi\pi^*$ state which is located *ca.* 6000 cm^{-1} below that of $Na_3[Gd(L^1 - 2H)_3]$. The lifetime of the $^3\pi\pi^*$ state emission, 1.54 ms (H_2O), is also substantially affected by the substitution of the pyridine being ten times shorter than in $Cs_3[Gd(L^1 - 2H)_3]$.[14b]

In contrast, the ligand based singlet and triplet state emissions completely disappear in the Eu^{III} triple-helical edifice while the typical line emission arising from the metal ion is observed (Fig. 5), indicating sensitisation of the metal ion *via* a $^3\pi\pi^*$-to-metal energy transfer. In methanol, the metal-centred emission is dominated by the $^5D_0 \rightarrow {}^7F_2$ transition, as shown by the integrated and corrected relative intensities of the $^5D_0 \rightarrow {}^7F_J$ transitions: 0.01, 1.00, 10.07, 0.09 and 1.55 for $J = 0, 1, 2, 3$ and 4, respectively. There is a single, very weak, $^5D_0 \rightarrow {}^7F_0$ transition located at 17 221 cm^{-1}, in line with the presence of a single Eu^{III} co-ordination environment. The emission spectrum (*cf.* Table S5, ESI) may be interpreted in terms of a pseudo-D_3 symmetry, in agreement with the NMR data: the $^5D_0 \rightarrow {}^7F_0$ transition is very weak (forbidden in D_3), there are two components for the transition to $^7F_1$ (allowed $A_1 \longrightarrow A_2$ and $A_1 \longrightarrow E$ transitions) and two components for the transition to $^7F_2$ (two allowed $A_1 \longrightarrow E$ transitions). The lifetime of the $^5D_0$(Eu) state is short, amounting to 0.177(4) ms, and the absolute quantum yield of the Eu^{III}-centred luminescence upon excitation through the ligand levels is 0.09%. In water, the emission spectrum is of much weaker intensity, the $^5D_0$ lifetime dropping to *ca.* 0.02 ms (compared to 1.67 ms for $[Eu(L^1 - 2H)_3]^{3-}$ in the same conditions)[43] and a residual emission from the ligand $^1\pi\pi^*$ is seen. It is known that an efficient ligand-to-metal energy transfer requires a good $^1\pi\pi^* \longrightarrow {}^3\pi\pi^*$ intersystem crossing, which is maximised when the energy difference between these states is close to 5000 cm^{-1}.[44] In our case, $\Delta E(^1\pi\pi^* - {}^3\pi\pi^*)$ amounts to 1458 and 577 cm^{-1} in methanol and water, respectively, and is therefore too small. Moreover, the energy difference between the 0-phonon band of the $^3\pi\pi^*$ emission and the $^5D_0$ level, 337 (H_2O) and 980 cm^{-1} (MeOH) as determined at 77 K, is also very small. This further explains the poor sensitisation of the Eu^{III} complex both in water and in methanol, as well as the short lifetime of the $^5D_0$ level, a back transfer process onto the ligand being possible.

A high resolution luminescence study has been performed at low temperature (10 K) on a solid sample of $Cs_3[Eu(L^4 - 2H)_3]$ to gain information on the chemical environment of the metal ion. Upon excitation in the ligand $^1\pi\pi^*$ state the integrated and corrected relative intensities of the $^5D_0 \longrightarrow {}^7F_J$ transitions are comparable to those measured for the solution in methanol: 0.04, 1.00, 6.98, 0.08 and 0.95 for J = 0, 1, 2, 3 and 4, respectively. The very weak $^5D_0 \longrightarrow {}^7F_0$ transition occurs at 17 218 cm^{-1}; it is very broad (full width at half height fwhh = 46 cm^{-1}) and unsymmetrical on its high energy side, pointing to somewhat different environments for the Eu^{III} ions most probably resulting from crystal defects. The emission spectrum may again be interpreted in terms of a severely distorted D_3 symmetry (*cf.* Table S4, ESI): the $^7F_1$ sublevel is split into one singlet and one closely spaced doublet (31 cm^{-1}), while the $^7F_2$ level is split into one singlet and two doublets. Using the correlation proposed between the energy ν of the $^5D_0 \longrightarrow {}^7F_0$ transition at 295 K and the ability of the co-ordinating atoms to produce a nephelauxetic effect δ, $\nu - \nu_0 = C_{CN}\Sigma_i n_i \delta_i$, with $C_{CN} = 1$, $\nu_0 = 17\,374$ cm^{-1} $\delta_{CO} = -17.2$, and $\delta_{Npy} = -12.1$,[45] we obtain $\nu = 17\,235$ cm^{-1} a value which roughly matches the experimental value of 17 230 cm^{-1} for $Cs_3[Eu(L^4 - 2H)_3]$ (recalculated at 295 K with a dependence of 1 cm^{-1} per 24 K).

Since L^4 possesses a low-energy triplet state, it appears that it would be suited for sensitisation of the Yb^{III} ion,[46] the energy difference between the ligand triplet state and the metal $^2F_{5/2}$ excited state being around 7000 cm^{-1}. The luminescence spectrum of the $Cs_3[Yb(L^4 - 2H)_3]$ compound, recorded in the solid state at 295 K under excitation through the ligand levels, indeed consists of an intense band centred at 10 233 cm^{-1} (fwhh = 119 cm^{-1}), assigned to the $^2F_{5/2} \longrightarrow {}^2F_{7/2}$ transition. Therefore, in spite of the small $\Delta E(^2F_{5/2} - {}^2F_{7/2})$ gap, which favours non-radiative deactivation processes, ligand L^4 acts as a good antenna for Yb^{III}.

Conclusion

The introduction of an alkyne substituent in the 4-position of the pyridine ring in ligand L^4 is obtained with good overall yield. Under stoichiometric conditions, triple-stranded helicates $[Ln(L^4 - 2H)]^{3-}$ are formed in methanol and water, the stability of which in the latter solvent is fairly large, although lower than that of the $[Ln(L^1 - 2H)_3]^{3-}$ complexes, probably because of the large electron delocalisation onto the π system of the ligand and/or partial protonation of the terminal amino groups. The solution structure determined in water by paramagnetic NMR measurements shows the Ln^{III} ions being nine-co-ordinated with a chemical environment close to that observed for the $[Ln(L^1 - 2H)_3]^{3-}$ complexes in the solid state. The introduction of the 4-aminophenylethynyl substituent drastically shifts the energy of the $^3\pi\pi^*$ state of the ligand toward lower energies, resulting in a poor sensitisation of Eu^{III}, but allows an efficient energy transfer onto Yb^{III} which emits in the near infrared. The 4-aminophenylethynyl substituent is one of the groups commonly used for coupling luminescent stains to biological materials[47] so that the presently developed synthetic technology will enable us to produce adequate lanthanide-containing building blocks for the design of luminescent probes, provided the problem of the (too) low lying triplet state can be solved.

Acknowledgements

This work is supported by grants from the Swiss National Science Foundation and by the Swiss Office for Education and Science (COST action D18). We thank Veronique Foiret for her help in recording high resolution luminescence spectra and lifetimes and Dr M. Elhabiri and Mr M. Hollenstein for preliminary work towards the synthesis of the ligand.

References

1 J.-C. G. Bünzli, in *Rare Earths*, ed. R. Saez-Puche and P. Caro, Editorial Complutense, Madrid, 1998, p. 223ff.

2 (*a*) R. B. Lauffer, in *MRI Clinical Magnetic Resonance Imaging*, ed. R. R. Edelman M. B. Zlatkin and J. R. Hesselink, W. B. Saunders Co., Philadelphia, 2nd ed., 1996, vol. 1, ch. 5; (*b*) P. Caravan, J. J. Ellison, T. J. McMurry and R. B. Lauffer, *Chem. Rev.*, 1999, **99**, 2293.

3 (*a*) T. C. Bruice, A. Tsubouchi, R. O. Dempey and L. P. Olson, *J. Am. Chem. Soc.*, 1996, **118**, 9867; (*b*) P. Hurst, B. K. Takasaki and J. Chin, *J. Am. Chem. Soc.*, 1996, **118**, 9982.

4 (*a*) G. L. DeNardo, G. R. Mirik, L. A. Kroger, R. T. O'Donnel, C. F. Meares and S. J. De Nardo, *J. Nucl. Med.*, 1996, **37**, 451; (*b*) M. J. Heeg and S. S. Jurisson, *Acc. Chem. Res.*, 1999, **32**, 1053.

5 V. W. W. Yam and K. K. W. Lo, *Coord. Chem. Rev.*, 1999, **184**, 157.

6 D. E. Koshland, Jr., *Angew. Chem., Int. Ed. Engl.*, 1994, **33**, 2375.

7 C. Piguet and J.-C. G. Bünzli, *Chem. Soc. Rev.*, 1999, **28**, 347.

8 F. Renaud, C. Piguet, G. Bernardinelli, J.-C. G. Bünzli and G. Hopfgartner, *Chem. Eur. J.*, 1997, **3**, 1646 and 1661.

9 C. Piguet, J.-C. G. Bünzli, G. Bernardinelli, G. Hopfgartner and A. F. Williams, *J. Am. Chem. Soc.*, 1993, **115**, 8197; N. Martin, J.-C. G. Bünzli, V. McKee, C. Piguet and G. Hopfgartner, *Inorg. Chem.*, 1998, **37**, 577.

10 C. Platas, M. Elhabiri, M. Hollenstein, J.-C. G. Bünzli and C. Piguet, *J. Chem. Soc., Dalton Trans.*, 2000, 2031.

11 M. Elhabiri, R. Scopelliti, J.-C. G. Bünzli and C. Piguet, *J. Am. Chem. Soc.*, 1999, **121**, 10747.

12 C. Edder, C. Piguet, G. Bernardinelli, J. Mareda, C. G. Bochet, J.-C. G. Bünzli and G. Hopfgartner, *Inorg. Chem.*, 2000, **39**, 5059.

13 S. Rigault, C. Piguet, G. Bernardinelli and G. Hopfgartner, *Angew. Chem., Int. Ed.*, 1998, **27**, 169.

14 (*a*) I. Grenthe, *J. Am. Chem. Soc.*, 1961, **83**, 360; (*b*) P. A. Brayshaw, J.-C. G. Bünzli, P. Froidevaux, J. M. Harrowfield, Y. Kim and A. N. Sobolev, *Inorg. Chem.*, 1995, **34**, 2068; (*c*) J. M. Harrowfield, Y. Kim, B. W. Skelton and A. H. White, *Aust. J. Chem.*, 1995, **48**, 807; (*d*) C. N. Reilley, B. W. Good and J. F. Desreux, *Anal. Chem.*, 1975, **47**, 2110; (*e*) E. Huskowska and J.-P. Riehl, *Inorg. Chem.*, 1995, **34**, 5615.

15 (*a*) F. Renaud, C. Piguet, G. Bernardinelli, J.-C. G. Bünzli and G. Hopfgartner, *Chem. Eur. J.*, 1997, **3**, 1646; (*b*) F. Renaud, C. Piguet, G. Bernardinelli, J.-C. G. Bünzli and G. Hopfgartner, *Chem. Eur. J.*, 1997, **3**, 1660.

16 G. Muller, B. Schmidt, J. Jiricek, G. Hopfgartner, J. P. Riehl, J.-C. G. Bünzli and C. Piguet, *J. Chem. Soc., Dalton Trans.*, 2001, 2655.

17 J. B. Lamture, Z. H. Zhou, A. S. Kumar and T. G. Wensel, *Inorg. Chem.*, 1995, **34**, 864.

18 E. R. Malinowski and D. G. Howery, *Factor Analysis in Chemistry*, J. Wiley, New York, Chichester, Brisbane and Toronto, 1980.

19 H. Gampp, M. Maeder, C. J. Meyer and A. D. Zuberbühler, *Talanta*, 1986, **33**, 943.

20 P. K. Glasoe and F. A. Long, *J. Phys. Chem.*, 1960, **64**, 188.

21 C. Piguet, A. F. Williams, G. Bernardinelli, E. Moret and J.-C. G. Bünzli, *Helv. Chim. Acta*, 1992, **75**, 1697.

22 S. Petoud, T. Glanzmann, J.-C. G. Bünzli, C. Piguet, X. Qin and R. P. Thummel, *J. Lumin.*, 1999, **82**, 69.

23 S. R. Meech and D. Phillips, *J. Photochem.*, 1983, **23**, 193.

24 H. Takalo, J. Kankare and E. Hänninen, *Acta Chem. Scand., Ser. B*, 1988, **42**, 448.

25 C. A. Grob and H. R. Pfaendler, *Helv. Chim. Acta*, 1971, **54**, 2060.

26 J. F. Desreux, in *Lanthanide Probes in Life, Chemical and Earth Sciences*, ed. J.-C. G. Bünzli and G. R. Choppin, Elsevier Science Publishers B. V., Amsterdam, 1989, ch. 2.

27 W. C. Wolsey, *J. Chem. Educ.*, 1973, **50**, A335.

28 (*a*) K. Sonogashira, Y. Tohda and N. Hagihara, *Tetrahedron Lett.*, 1975, **50**, 4467; (*b*) H. A. Diek and F. R. Heck, *J. Organomet. Chem.*, 1975, **93**, 259.

29 M. R. Lewis, D. W. Deerfield, R. A. Hoke, K. A. Koehler, L. G. Pedersen and R. G. Hiskey, *J. Biol. Chem.*, 1988, **263**, 1358.

30 R. M. Tichane and W. E. Bennett, *J. Am. Chem. Soc.*, 1957, **79**, 1293.

31 B. Perlemutter-Hayman, *Acc. Chem. Res.*, 1986, **19**, 90.

32 J. A. Peters, J. Huskens and D. J. Raber, *Prog. NMR Spectrosc.*, 1996, **28**, 283; J. H. Forsberg, in *Handbook on the Physics and Chemistry of Rare Earths*, ed. K. A. Gschneidner, Jr. and L. Eyring, Elsevier Science Publishers B.V., Amsterdam, 1996, vol. 23, ch. 153, p. 1ff.

33 A. D. Sherry C. F. G. C. Geraldes, in *Lanthanide Probes in Life, Chemical and Earth Sciences*, ed. J.-C. G. Bünzli and G. R. Choppin, Elsevier Science Publishers B. V., Amsterdam, 1989, ch. 4.

34 C. N. Reilley, B. W. Good and J. F. Desreux, *Anal. Chem.*, 1975, **47**, 2110.

35 (*a*) R. M. Golding and M. P. Halton, *Aust. J. Chem.*, 1972, **25**, 2577; (*b*) A. A. Pinkerton, M. Rossier and S. Stavros, *J. Magn. Reson.*, 1985, **64**, 420.

36 B. Bleaney, *J. Magn. Reson.*, 1972, **8**, 91.

37 J. Ren and D. Sherry, *J. Magn. Reson., Ser. B*, 1996, **111**, 178; J. Reuben, *J. Magn. Reson.*, 1982, **50**, 233.

38 C. Platas, F. Avecilla, A. de Blas, C. F. G. C. Geraldes, T. Rodriguez-Blas, H. Adams and J. Mahia, *Inorg. Chem.*, 1999, **38**, 3190.

39 S. Rigault, C. Piguet and J.-C. G. Bünzli, *J. Chem. Soc., Dalton Trans.*, 2000, 2045.

40 (*a*) D. P. Glover-Fischer, D. H. Metcalf, T. A. Hopkins, V. J. Pugh, S. J. Chisdes, J. Kankare and F. S. Richardson, *Inorg. Chem.*, 1998, **37**, 3026; (*b*) S. D. Belair, C. L. Maupin, M. W. Logue and J. P. Riehl, *J. Lumin.*, 2000, **86**, 61.

41 Cerius-2, version 3.0, Molecular Simulations Inc., San Diego, USA, 1997.

42 J. H. Forsberg, R. M. Delaney, Q. Zhao, G. Harakas and R. Chandran, *Inorg. Chem.*, 1995, **34**, 3705.

43 Y. An, M. T. Berry and F. C. J. M. van Veggel, *J. Phys. Chem. A*, 2000, **104**, 11243.

44 F. J. Steemers, W. Verboom, D. N. Reinhoudt, E. B. Vandertol and J. W. Verhoeven, *J. Am. Chem. Soc.*, 1995, **117**, 9408.

45 S. T. Frey and W. DeW. Horrocks, Jr., *Inorg. Chim. Acta*, 1995, **229**, 383.

46 C. Platas, F. Avecilla, A. de Blas, T. Rodriguez-Blas, C. F. G. C. Geraldes, E. Tóth, A. E. Merbach and J.-C. G. Bünzli, *J. Chem. Soc., Dalton Trans.*, 2000, 611.

47 I. Hemmilä, T. Ståhlberg and P. Mottram, *Bioanalytical Applications of Labelling Technologies*, Wallac Oy, Turku, 2nd edn., 1995.